CASE FILE
COPY

COLD-FLOW PERFORMANCE OF SEVERAL VARIATIONS OF A RAM-AIR-COOLED PLUG NOZZLE FOR SUPERSONIC-CRUISE AIRCRAFT

by Douglas E. Harrington, Stanley M. Nosek,
and David M. Straight

Lewis Research Center
Cleveland, Ohio 44135

1. Report No. NASA TM X-3110	2. Government Accession No.	3. Recipient's Catalog No.
4. Title and Subtitle COLD-FLOW PERFORMANCE OF SEVERAL VARIATIONS OF A RAM-AIR-COOLED PLUG NOZZLE FOR SUPERSONIC-CRUISE AIRCRAFT		5. Report Date OCTOBER 1974
		6. Performing Organization Code
7. Author(s) Douglas E. Harrington, Stanley M. Nosek, and David M. Straight		8. Performing Organization Report No. E-7975
9. Performing Organization Name and Address Lewis Research Center National Aeronautics and Space Administration Cleveland, Ohio 44135		10. Work Unit No. 501-24
		11. Contract or Grant No.
12. Sponsoring Agency Name and Address National Aeronautics and Space Administration Washington, D.C. 20546		13. Type of Report and Period Covered Technical Memorandum
		14. Sponsoring Agency Code

15. Supplementary Notes

16. Abstract

Experimental data were obtained with a 21.59-cm (8.5-in.) diameter cold-flow model in a static altitude facility to determine the thrust and pumping characteristics of several variations of a ram-air-cooled plug nozzle. Tests were conducted over a range of nozzle pressure ratios simulating supersonic cruise and takeoff conditions. Primary throat area was also varied to simulate afterburner on and off. Effect of plug size, outer shroud length, primary nozzle geometry, and varying amounts of secondary flow were investigated. At a supersonic cruise pressure ratio of 27, nozzle efficiencies were 99.7 percent for the best configurations.

17. Key Words (Suggested by Author(s)) Nozzles; Plug nozzles; Exhaust nozzles; Nozzle design; Nozzle geometry; Nozzle performance; Plug nozzle cooling; Propulsion	18. Distribution Statement Unclassified - unlimited Category 28		
19. Security Classif. (of this report) Unclassified	20. Security Classif. (of this page) Unclassified	21. No. of Pages 36	22. Price* $3.25

COLD FLOW PERFORMANCE OF SEVERAL VARIATIONS OF A RAM-AIR-COOLED

PLUG NOZZLE FOR SUPERSONIC-CRUISE AIRCRAFT

by Douglas E. Harrington, Stanley M. Nosek, and David M. Straight

Lewis Research Center

SUMMARY

An experimental study was conducted to determine the thrust and pumping charac-
teristics of several variations of a ram-air-cooled plug nozzle. This study was con-
ducted in a static cold-flow altitude facility with a 21.59-centimeter (8.5-in.) diameter
model. The range of nozzle pressure ratios simulated supersonic cruise and takeoff
conditions. Primary throat area was also varied to simulate afterburner on and off.
Effect of plug size, outer shroud length, primary nozzle geometry, and varying amounts
of secondary flow were investigated.

With the configurations simulating afterburner off and the outer shroud extended,
nozzle efficiencies for both the intermediate and large plugs with the cylindrical outer
primary were 99.7 percent at a supersonic cruise pressure ratio of 27. The perform-
ance at this pressure ratio did not vary appreciably over a range of inner and outer cor-
rected secondary weight flows from 2 to 5 percent. The small plug resulted in a de-
crease in nozzle efficiency to approximately 99 percent. A conical 10° outer primary
with the intermediate plug had a 1.3-percent reduction in efficiency to 98.4 percent.
The high levels of efficiency for two typical nozzles tested were confirmed by component
force analyses. At a typical climb-out pressure ratio of 4.0 with the outer shroud re-
tracted, the highest efficiency (98.4 percent) was obtained with the large plug and the
cylindrical outer primary.

With the configurations simulating afterburner on, variations in plug size had little
effect on nozzle efficiency at a typical acceleration nozzle pressure ratio of 22. With
the outer shroud extended, nozzle efficiency for all three plug sizes was approximately
98.3 percent. At a climb-out pressure ratio of 4.0 with a fully retracted outer shroud,
the highest efficiency (97.8 percent) occurred with the intermediate plug.

INTRODUCTION

Aircraft designed for long range flight at supersonic speeds must maintain high propulsion system efficiency during the entire mission. A plug nozzle used in conjunction with an afterburning engine would provide high performance over a wide range of operating conditions (refs. 1 to 7). However, one of the problems associated with the plug nozzle is properly designing it to operate in the high-temperature environment of the engine exhaust during afterburning operation. A number of cooling schemes applicable to exhaust nozzles are reported in references 8 to 10. Of the various schemes proposed, film cooling with air is most commonly used. Results from a number of film-cooling investigations on plug nozzles are reported in references 11 to 13.

In reference 1 a new plug-nozzle cooling concept (see fig. 1, herein) was introduced in which external or engine-inlet ram air is used for film cooling the plug. This concept is essentially a modification of the plug nozzle reported in reference 2. That particular nozzle used a translating outer shroud and demonstrated high efficiencies (approx. 99.5 percent) over a wide range of nozzle pressure ratios. Both nozzles are basically the same except that the ram-air-cooled plug (ref. 1) uses slots for film cooling the plug and outer shroud. Using ram-air for cooling rather than compressor-bleed air may result in a lower thrust penalty. Part of the relatively low-energy ram air from the inlet is ducted through crossover struts upstream of the afterburner and then to a large flow passage ahead of the plug. The cooling air then enters an annulus surrounding the plug.

To investigate further the potential of this concept, an experimental study was conducted. This investigation was essentially a continuation of the testing reported in reference 1 in which only a few configurations were tested. In the present study more variations of the basic concept were investigated. Testing was conducted in a static cold-flow altitude facility with a 21.59-centimeter (8.5-in.) diameter model. Thrust and pumping characteristics were determined for several variations of this nozzle. The effect of plug size, outer shroud length, primary nozzle geometry, and varying amounts of secondary flow were investigated. Dry air at room temperature was provided for both primary and secondary air flows. Nozzle pressure ratios from 3.0 (takeoff) to 27 (supersonic cruise) were investigated. Inner secondary flow (plug coolant) was varied from 0 to 8 percent of primary flow, and outer secondary flow (shroud coolant) was from 0 to 6 percent.

SYMBOLS

A_{is} inner secondary flow area at primary lip (fig. 5(a))

A_{os} outer secondary flow area (fig. 5(a))

A_{lip} primary nozzle flow area in lip plane (fig. 5(a))

A_8 primary nozzle throat area (fig. 5(a))

A_9 flow area between end of extended outer shroud and plug surface (fig. 5(a))

d_m model diameter

F_c calculated gross thrust (stream momentum, and pressure forces; fig. 9) excluding friction

F_i sum of ideal isentropic thrusts (primary and two secondaries)

F_{ip} ideal isentropic thrust of primary stream

F_{is} inner secondary component forces (stream momentum and pressure forces; including pressure force on inner surface of inner primary; fig. 9)

F_m measured gross thrust (based on load cell)

F_{os} outer secondary component forces (stream momentum and pressure forces; fig. 9)

F_p primary stream component forces (stream momentum and pressure forces at primary lip plane; fig. 9)

F_{pl} plug-surface pressure force (downstream of plug maximum diameter; fig. 9)

P_0 static pressure in test chamber

$P_{t,is}$ inner secondary total pressure at station 7

$P_{t,os}$ outer secondary total pressure at station 7

$P_{t,7}$ primary total pressure at station 7

T_{is} inner secondary-air total temperature

T_{os} outer secondary-air total temperature

T_p primary-air total temperature

W_{is}	inner secondary airflow rate
W_{os}	outer secondary airflow rate
W_p	primary airflow rate
σ	standard deviation
x	axial distance downstream from inner primary lip
$\omega_{is}\sqrt{\tau_{is}}$	corrected inner secondary flow ratio, $(W_{is}/W_p)\sqrt{T_{is}/T_p}$
$\omega_{os}\sqrt{\tau_{os}}$	corrected outer secondary flow ratio, $(W_{os}/W_p)\sqrt{T_{os}/T_p}$

APPARATUS AND PROCEDURE

Installation

A photograph and a schematic of a typical test nozzle installed in the static test facility are shown in figures 2 and 3. The nozzle was attached by an adapter to a section of pipe rigidly mounted on a bedplate. The bedplate was freely suspended by four flexure rods. The metric portion of the installation (bedplate, adapter, nozzle, etc.) was connected to the grounded primary-air bellmouth by means of a flexible bellows. Forces acting on the metric section were measured with a load cell mounted between the bedplate and a grounded portion of the facility. Measured nozzle gross thrust F_m was then determined from the load cell measurement, primary inlet momentum, and several facility tare forces.

Facility Calibration

Nozzle primary mass flow was calculated from pressure and temperature measurements taken upstream of the bellmouth at the primary-air metering station. Bellmouth flow coefficients were determined with two ASME calibration nozzles. One of these nozzles had a throat area that corresponded to cruise (afterburner off); the other corresponded to acceleration (afterburner on). Inner and outer secondary mass flows were measured with standard ASME flow metering orifices located in external supply lines.

The ASME nozzles were also used to calibrate the thrust of the metric portion of the installation. This was done before testing the ram-air-cooled plug nozzles. The calibration data generated for the afterburner-off configurations is presented in figure 4(a). The gross thrust coefficient calculated from the measured thrust is plotted as

a function of the nozzle pressure ratio and compared with the theoretical thrust coeffi-
cient. Practically all of the points fall within ±1/2 percent of deviation from the theoret-
ical. The standard deviation for these data was 0.0028. Calibration data generated for
the afterburner-on configurations are presented in figure 4(b). As before, the majority
of the data fall within ±1/2 percent of deviation from the theoretical. The standard de-
viation for these data was 0.0018.

The calibration results do not include the effect of bringing secondary air onto the
metric section. As was reported in reference 1, the bourdon tube effect of the flexible
secondary-air lines may have induced some inaccuracies, causing some of the measured
nozzle efficiencies to exceed 100 percent. However, for this test the rubber secondary-
air lines were replaced with lines incorporating solid pipe and bellows (two flexible steel
bellows in each line). In addition, the secondary air was brought on normal to the
metric section centerline to minimize any interactions in the thrust direction. A pres-
sure calibration of the secondary lines was also performed to determine the effect that
pressurizing the air lines has on thrust. Although relatively small, this effect was
accounted for in measuring nozzle gross thrust.

Nozzle Configurations

Geometric details of the test nozzles are shown in figures 5 to 7. Important area
ratios are listed in table I. The variation of inner secondary flow area A_{is} was simu-
lated by using three different plug sizes (see fig. 5). The plug was supported by three
struts equally spaced circumferentially. The details of a typical support strut are shown
in section A-A of figure 5(a). Figure 5(b) shows the various outer shroud lengths that
were tested. As in reference 1, the lip of the large inner primary was chosen as the
nozzle reference point (X = 0). This reference point was the same for all nozzles.

Two concepts of varying primary throat area for simulating afterburner operation
were tested. (See fig. 6.) One concept simulated primary area variations by using two
different fixed inner primary shrouds with the same cylindrical outer primary shroud
(fig. 6(a)). Afterburner-off operation was simulated by using the large inner primary.
To simulate afterburner-on operation, the small inner primary was used. In both cases
the primary flow had some internal expansion corresponding to a pressure ratio of
approximately 3.0. Figure 6(b) depicts the other concept of primary throat area varia-
tion. Simulation of primary throat area variation with this concept was accomplished
by using two different fixed outer primary shrouds and a single inner primary shroud
(small inner primary).

Afterburner-off operation was simulated by using a 10° conical outer primary. In
this mode no internal expansion of the primary flow was obtained. Afterburner-on oper-

ation was simulated as before by using the small inner primary and the cylindrical outer primary.

Details of the inner primary shrouds are shown in figure 7. Both primaries had large radii of curvature to minimize sonic line distortion at the throat. In addition, the trailing edge angles of the inner primary boattails were 10° on the primary flow side and 5° on the inner secondary flow side.

Model Instrumentation

Figure 8 presents the instrumentation that was used on the model. The instrumentation at station 7 (fig. 8(a)) was used to determine the flow properties of the various streams as they entered the nozzle. All total-pressure rakes were equal-area weighted, and the static-pressure orifices were offset circumferentially from the rakes to minimize disturbances from these rakes. The static-pressure orifices for determining component forces and pressure distributions are shown in figure 8(b). In addition to these static-pressure orifices, four pressures (not shown in fig.) were measured on the 10° conical outer primary to assist in determining the component force on that primary.

Procedure

Nozzle pressure ratios were set by maintaining a constant nozzle inlet pressure $P_{t,7}$ and varying the tank pressure P_0 with the exhausters. Each of the nozzle configurations was tested over a range of pressure ratios encompassing the design conditions. Design conditions corresponded to a pressure ratio of 3.0 (takeoff) and 27 (supersonic cruise). Inner secondary weight flow ratio $(\omega_{is}\sqrt{\tau_{is}})$ was varied from 0 to 8 percent, and the outer secondary weight flow ratio $(\omega_{os}\sqrt{\tau_{os}})$ was varied from 0 to 6 percent.

Thrust Calculations

The ideal jet thrust for each of the primary and secondary flows was calculated from the measured mass flow rate expanded from its measured total pressure to tank static pressure P_0. Nozzle efficiency is then defined as the ratio of the gross thrust to the sum of the ideal thrusts of both primary and secondary flows:

$$\text{Nozzle efficiency} = \frac{F_m}{F_i} \text{ or } \frac{F_c}{F_i}$$

In addition, the measured nozzle gross thrust coefficient was also calculated. It is defined as the ratio of the measured gross thrust to the ideal thrust of the primary flow:

$$\text{Nozzle gross thrust coefficient} = \frac{F_m}{F_{ip}}$$

The calculated gross thrust F_c was determined by summing the stream thrusts of all three flows and the aft plug pressure force. A component force summary is depicted in figure 9. The calculated gross thrust does not include losses due to internal friction or drag from the plug support struts. However, estimates of the friction force were made at the design pressure ratio of 27 using two different boundary-layer methods (refs. 14 and 15). The measured gross thrust F_m was determined from a load cell measurement, primary inlet momentum, and several facility tare forces.

RESULTS AND DISCUSSION

The initial summary figures (figs. 10 to 16) present comparisons between most of the nozzle configurations tested. For these summary figures data are presented at corrected inner and outer secondary weight flows of 5 and 3 percent, respectively. These values were chosen as being representative of the approximate cooling flows needed for a primary gas temperature of 1944 K (3500° R; ref. 1). In figures 10 to 13, the discussion is centered around the design points of takeoff and supersonic cruise. In figures 14 to 16 a correlation of pumping characteristics for all nozzles tested over a wide range of pressure ratios will be discussed. Nozzle performance data are presented in figures 17 to 20. The effect of outer shroud length, outer primary shape, and varying both inner and outer secondary flows will be shown in those figures.

Effect of Plug Size

The effect of plug size on nozzle performance characteristics for the afterburner-off configurations is shown in figure 10. At a supersonic cruise pressure ratio of 27, nozzle efficiencies were 99.7 percent for both the intermediate and large plugs with the cylindrical outer primary and the outer shroud fully extended ($x/d_m = 0.82$). The small plug decreased the nozzle efficiency to about 99 percent. At the same pressure ratio the intermediate plug with the 10° conical outer primary had an efficiency of 98.4 percent. This corresponds to a 1.3-percent loss in nozzle efficiency when compared with the intermediate plug with the cylindrical outer primary. A more complete discussion of this performance loss is given when figure 18 is discussed.

With the cylindrical outer shroud fully retracted (x/d_m = -0.16) nozzle efficiencies for the larger plugs were sensitive to plug size. At a climb-out pressure ratio of 4.0 a thrust efficiency of 98.4 percent was obtained with the large plug and cylindrical outer primary. However, with the intermediate plug, nozzle efficiency dropped to 97.8 percent. These efficiencies are somewhat less than 99+ percent efficiency reported for a similar nozzle without inner secondary flow (ref. 2). The lower efficiencies can probably be attributed to the discontinuity caused by the inner secondary cooling slots on the plug. At an assumed takeoff pressure ratio of 3.0, nozzle efficiencies were lower than at a pressure ratio of 4.0 and were similarly sensitive to plug size. These nozzles had cylindrical outer primaries designed to have internal area ratios corresponding to a pressure ratio of approximately 3.0. However, from the low efficiencies, it is apparent these nozzles were actually overexpanded at a pressure ratio of 3.0. Further verification of this can be seen in figure 17.

The effect of plug size on nozzle performance characteristics for the afterburner-on nozzles is shown in figure 11. Variations in plug size had little effect on nozzle efficiency at an acceleration nozzle pressure ratio of 22. With the outer shroud fully extended (x/d_m = 0.82), nozzle efficiency for all three plug sizes was approximately 98.3 percent. These peak efficiencies were approximately 1.4 percent lower than the values obtained with the afterburner-off configurations (fig. 10). At an assumed climb-out pressure ratio of 4.0 with a fully retracted outer shroud (x/d_m = -0.16), the highest efficiency (97.8 percent) occurred with the intermediate plug.

The lower value of efficiency for the large plug may have been a result of the large inner-secondary pressure required due to slot choking. The trend in efficiency at an assumed takeoff pressure ratio of 3.0 was similar to the trend at the climb-out pressure ratio of 4.0. The highest efficiency (97.4 percent) was again obtained with the intermediate plug.

As would be expected the pressure required to pump 5 percent inner secondary flow (plug coolant) increased with plug size for the afterburner-on nozzles. This was true, not only at low pressure ratios with a fully retracted shroud, but also at a pressure ratio of 22 with a fully extended shroud. In particular, the large plug causes choking on the inner slot and required such a large amount of pressure to pump the 5 percent plug-coolant flow that use of the large plug with ram air would probably not be feasible. The pumping characteristics of the outer secondary flow, on the other hand, were completely independent of plug size.

Comparison of Calculated and Measured Nozzle Efficiencies

A comparison of measured and calculated nozzle efficiencies for two nozzles typical of those tested is presented in figure 12. Data are shown for the intermediate plug

with a fully extended outer shroud ($x/d_m = 0.82$) and the afterburner off. Although data are presented for only two nozzle configurations, the results are representative of all nozzles tested. An estimate of the internal friction force was made at the design pressure ratio of 27 and reduced the efficiency by about a 1/2 percent. This reduction in efficiency was used to adjust the calculated efficiency at a pressure ratio of 27.

For both the cylindrical and 10° conical primary, calculated nozzle efficiencies were approximately 1/2 percent to $1\frac{1}{2}$ percent higher than the measured efficiencies over a range of pressure ratios from 10 to 27. However, at a pressure ratio of 27 the calculated efficiency adjusted for estimated internal friction showed good agreement with the measured efficiency for both outer primaries. This analysis tends to confirm the high levels of efficiency that were measured for some of the typical nozzle configurations.

Pumping Characteristics

The inner-secondary flow pressure-recovery requirements are presented in figure 13. Data are shown at an assumed takeoff pressure ratio of 3.0 and a corrected outer secondary flow of 3 percent. The outer shroud was fully retracted. Afterburner-off configurations with both the small and intermediate plug sizes pumped 5 percent corrected inner secondary flow at 0.95 secondary-to-ambient pressure ratio. Afterburner-on configurations with both the small and intermediate plugs were capable of pumping approximately 3 percent corrected inner secondary flow at 0.95 secondary-to-ambient pressure ratio. The large plug configuration (afterburner on) would not be a good candidate for ram-air-cooling application because such large pressures were necessary to pump even small quantities of inner secondary air.

The pumping data for the various configurations tested were plotted separately for the inner and outer secondary flow streams in figures 14 to 16 as a function of an area ratio parameter. This parameter is the sum of the primary- and secondary-discharge areas to the primary throat area (see fig. 5 and table I).

The pumping data for the inner secondary is shown in figure 14(a) and the outer secondary in figure 14(b) for nozzle pressure ratios greater than 5.0. The inner secondary pumping characteristics were independent of the length of the outer shroud, but the outer secondary pumping curves shown represent data from only the two most extended outer shrouds tested ($x/d_m = 0.35$ and 0.82). The high pressures at the low area ratios are caused by choking the secondary discharge area.

The pumping characteristics of the inner secondary at a takeoff nozzle pressure ratio of 3.0 is presented in figure 15. Conversely, the effect of nozzle pressure ratio ($P_{t,7}/P_0$ from 2 to 7) at a constant corrected inner secondary flow rate of 0.05 is shown in figure 16. The outer shroud was in the retracted position for these data except for a

few points shown in figure 16 (solid symbols) where the long shroud was used. Slightly improved pumping was obtained with the long shroud. However, operation of the nozzle with an extended shroud at a pressure ratio of 3.0 may result in poor thrust performance and potentially unstable flow due to separation.

In general, lower secondary pressure ratios are reached with larger values of the area ratio parameter, but the curves approach asymtotically zero slope at very large area ratios. Large area ratios also represent small plug sizes. Thus, configurations with improved pumping may have lower thrust efficiencies. A trade-off between pumping requirements for cooling and thrust performance is therefore indicated.

Effect of Outer Shroud Length

The effect of shroud length (over a range of nozzle pressure ratios) on nozzle performance characteristics is presented in figure 17. Data are shown for both afterburner-off and afterburner-on configurations. The outer-primary shroud was cylindrical. Corrected inner and outer secondary weight flows were 5 and 3 percent, respectively. Peak nozzle efficiencies occurred at lower nozzle pressure ratios for shorter outer-shroud lengths. These peak efficiencies occurred at area ratios (A_9/A_8) that were relatively close to ideal one-dimensional values. At intermediate pressure ratios $(P_{t,7}/P_0$ from 6 to 15), afterburner-on configurations generally had higher nozzle efficiencies than afterburner-off configurations.

These intermediate pressure ratios correspond to accelerations and climb flight conditions where the use of afterburning is maximized. In addition, peak efficiencies occur at lower pressure ratios with afterburner on than with afterburner off because of lower internal area ratios A_9/A_8 for a given outer shroud length.

Effect of Varying the Outer Primary

In varying the primary throat area for afterburner on or off operation, there is a choice of varying the area by either the inner or the outer primary flap (see fig. 6). Figure 18(a) shows the effect on nozzle performance when the two methods of throat area variation are used. When the outer primary is used for throat area variation (10° outer primary, afterburner off), a loss of 1 to $1\frac{1}{2}$ percent in efficiency occurs when compared with the cylindrical outer primary over the range of nozzle pressure ratios tested.

To determine where the loss in efficiency occurs, the momenta and pressure forces were calculated for each of the components; the primary stream, the secondary streams,

and the plug. The resultant component force analyses are presented in figure 18(b) for the afterburner-off configurations using the 10° conical primary and the cylindrical outer primary. The component forces presented in this figure are also schematically shown in figure 9. All of the component forces in figure 18(b) are presented as ratios to the total ideal thrust of the nozzle. When comparing the results at a nozzle pressure ratio of 27, typical of a supersonic cruise condition, it is noted that there is a 4-percent loss in the contribution by the primary flow when the 10° conical primary is used. Most of this loss can be attributed to the cosine of 10° flow deflection and the lack of flow expansion on the inner primary surface. However, part of this loss was recovered on the plug as can be seen by the plug force, which increased approximately $2\frac{1}{2}$ percent. In addition, the outer secondary contribution was increased by a 1/2 percent, and there was no change in the contribution by the inner secondary. Therefore, the net loss is then approximately 1 percent in efficiency as is shown in the plot of calculated efficiencies F_c/F_i. This calculated net loss is comparable to measured net loss, as shown in figure 18(a).

Secondary Flow Effects

The effect of inner secondary mass flow on nozzle performance characteristics is shown in figure 19. Data are presented for selected pressure ratios and shroud lengths at a corrected outer secondary weight flow of 3 percent. In general, nozzle efficiencies for the afterburner-off configurations were at their highest level and remained nearly constant at corrected inner secondary weight flows from 2 to 5 percent for a pressure ratio of 27. The outer shroud was extended to either $x/d_m = 0.82$ or 0.35. These efficiencies were approximately 99.7 percent for the large and intermediate plugs. However, even with no inner secondary flow the efficiencies remained about 99 percent for the nonafterburning case with an intermediate or large plug.

Nozzle efficiencies for the afterburner-on configurations at a pressure ratio of 22 and the outer shroud extended to $x/d_m = 0.82$ tended to peak at lower inner-secondary mass flows as plug size increased. With the outer shroud fully retracted ($x/d_m = -0.16$) and at a pressure ratio of 3, nozzle efficiencies for the afterburner-off configurations tended to increase with increasing rates of inner secondary weight flow. However, nozzle efficiencies for the afterburner-on configurations ($P_{t,7}/P_0 = 3$) tended to peak near a corrected inner-secondary weight flow of 5 percent.

The effect of outer secondary mass flow on nozzle performance characteristics is shown in figure 20. Data are presented for selected pressure ratios and shroud lengths at a corrected inner secondary weight flow of 5 percent. In general, with the cylindrical outer primary flap nozzle efficiencies for the afterburner-off configurations at a pres-

11

sure ratio of 27 and the outer shroud extended to $x/d_m = 0.82$ were relatively insensitive to variations in outer secondary mass flow from 2 to 6 percent. However, efficiencies dropped off noticeably when the outer secondary flow was reduced to zero. With the 10° conical outer primary, efficiencies increased with increasing outer secondary flow.

With the outer shroud fully retracted ($x/d_m = -0.16$) and at a pressure ratio of 3, nozzle efficiencies for all configurations generally peaked at zero outer secondary mass flow.

CONCLUDING REMARKS

This study has shown that the ram-air-cooled plug nozzle has the potential of high thrust performance. Used in conjunction with an afterburning turbojet it appears to be an attractive concept. In addition, a brief study of applying this concept to a duct burning turbofan engine indicated that the concept may also be applicable to other turbine engine cycles. Either ram-air or fan-discharge air could be used for cooling the plug in the turbofan cycle. Use of the fan-discharge air (or first or second stage bleed air in a turbojet) would provide higher cooling-air flow rates at the afterburning sea level takeoff condition. Whereas, the models tested in the present study may be marginal in providing enough air by ejector pumping.

Continued investigation of this nozzle concept appears desirable. Hot flow testing should be conducted to determine minimum cooling-air flow rates. Cycle and mission analysis should also be conducted to determine the trade-off factors between plug size, source of cooling air, and afterburning level. In addition, wind tunnel tests to determine external flow effects would be desirable.

SUMMARY OF RESULTS

An experimental study was conducted to determine the thrust and pumping characteristics of a plug nozzle similar to an earlier, high performing nozzle but incorporating slots on the plug and outer shroud for cooling with ram air. Tests were conducted in a static cold-flow altitude facility with a 21.59-centimeter (8.5-in.) diameter model over a range of nozzle pressure ratios simulating supersonic cruise and takeoff conditions. Primary throat area was also varied to simulate afterburner on and off. Effect of plug size, outer shroud length, primary nozzle geometry, and varying amounts of secondary flow were investigated. The following results were obtained:

Afterburner off -

1. At a supersonic cruise pressure ratio of 27 with the outer shroud extended,

12

nozzle efficiencies for both the intermediate and large plugs with the cylindrical outer primary were 99.7 percent. This performance did not vary appreciably over a range of inner and outer corrected secondary weight flow from 2 to 5 percent. The small plug resulted in a decrease in nozzle efficiency to about 99 percent. A conical 10° outer primary with the intermediate plug had a 1.3-percent reduction in efficiency to 98.4 percent.

2. The high levels of efficiency for two typical nozzles tested were confirmed by component force analyses.

3. With the cylindrical outer shroud fully retracted, nozzle efficiencies were sensitive to plug size. For example, at a typical climb-out pressure ratio of 4.0, a thrust efficiency of 98.4 percent was obtained with the large plug and cylindrical outer primary. However, with the intermediate plug at the same pressure ratio, nozzle efficiency dropped to 97.8 percent. These efficiencies are somewhat less than the 99+ percent efficiency reported for a similar nozzle without inner secondary flow.

Afterburner on –

1. Variations in plug size had little effect on nozzle efficiency at a typical acceleration nozzle pressure ratio of 22. With the outer shroud extended, nozzle efficiency for all three plug sizes was approximately 98.3 percent.

2. At a climb-out pressure ratio of 4.0 with a fully retracted outer shroud, the highest efficiency (97.8 percent) occurred with the intermediate plug. The same nozzle had an efficiency of 97.4 percent at a takeoff pressure ratio of 3.0. Corrected inner and outer secondary weight flow were 5 and 3 percent, respectively.

3. With the outer shroud fully retracted, both the small and intermediate plug nozzles were capable of pumping 3 percent corrected inner secondary flow at a secondary-to-ambient total-pressure ratio of 0.95.

Lewis Research Center,
    National Aeronautics and Space Administration,
        Cleveland, Ohio, June 21, 1974.

REFERENCES

1. Straight, David M.; Harrington, Douglas E.; and Nosek, Stanley M.: Experimental Cold-Flow Evaluation of a Ram-Air-Cooled Plug-Nozzle Concept for Afterburning Turbojet Engines. NASA TM X-2811, 1973.

2. Bresnahan, Donald L.; Johns, Albert L.: Cold Flow Investigation of a Low Angle Turbojet Plug Nozzle with Fixed Throat and Translating Shroud at Mach Numbers From 0 to 2.0. NASN TM X-1619, 1968.

3. Bresnahan, Donald L: Experimental Investigation of a 10° Conical Turbojet Plug Nozzle With Iris Primary and Translating Shroud at Mach Numbers From 0 to 2.0. NASA TM X-1709, 1968.

4. Bresnahan, Donald L.: Experimental Investigation of a 10° Conical Turbojet Plug Nozzle With Translating Primary and Secondary Shrouds at Mach Numbers From 0 to 2.0. NASA TM X-1777, 1969.

5. Johns, Albert L.: Quiescent-Air Performance of a Truncated Turbojet Plug Nozzle With Shroud and Plug Base Flows From a Common Source. NASA TM X-1807, 1969.

6. Harrington, Douglas E.: Performance of Convergent and Plug Nozzles at Mach Numbers From 0 to 1.97. NASA TM X-2112, 1970.

7. Harrington, Douglas E.: Performance of a 10° Conical Plug Nozzle With Various Primary Flap and Nacelle Configurations at Mach Numbers From 0 to 1.97. NASA TM X-2086, 1970.

8. Eckert, E.R.G.; and Livingood, John N.B.: Comparison of Effectiveness of Convection-, Transpiration-, and Film-Cooling Methods With Air as Coolant. NACA Rep. 1182, 1954.

9. Papell, S. Stephen; and Trout, Arthru M.: Experimental Investigation of Air Film Cooling Applied to An Adiabatic Wall By Means of an Axially Discharging Slot. NASA TN D-9, 1959.

10. Papell, S. Stephen: Effect of Gaseous Film Cooling of Coolant Injection Through Angled Slots and Normal Holes. NASA TN D-299, 1960.

11. Jeracki, Robert J.; and Chenoweth, Francis C.: Coolant Flow Effects on the Performance of a Conical Plug Nozzle at Mach Numbers From 0 to 2.0. NASA TM X-2076, 1970.

12. Chenoweth, Francis C.; and Lieberman, Arthur: Experimental Investigation of Heat-Transfer Characteristics of a Film-Cooled Plug Nozzle with Translating Shroud. NASA TN D-6160, 1971.

13. Clark, John S.; and Lieberman, Arthur: Thermal Design Study of an Air-Cooled Plug-Nozzle System for a Supersonic-Cruise Aircraft. NASA TM X-2475, 1972.

14. Elliot, David G.; Bartz, Donald R.; and Silver, Sidney: Calculation of Turbulent Boundary-Layer Growth and Heat Transfer in Axi-symmetric Nozzles. JPL-TR-32-387, Jet Propulsion Lab., California Institute of Technology, Feb. 15, 1963.

15. Spalding, D.B.; and Patankar, S.V.: Heat and Mass Transfer in Boundary Layer. Morgan-Grampian Books, Ltd., 1967.

TABLE I. - PERTINENT AREA RATIOS[a]

(a) Afterburner off; $A_8/A_m = 0.266$

Nozzle configuration		A_{pl}/A_m	A_{is}/A_m	A_{os}/A_m	A_{lip}/A_8	Area ratios					$\dfrac{A_{is} + A_{lip}}{A_8}$	$\dfrac{A_{os} + A_{lip}}{A_8}$
Type of outer primary shroud	Size of plug					A_9/A_8 (b)	A_9/A_8 (c)	A_9/A_8 (d)	A_9/A_8 (e)			
Cylindrical	Large	0.375	0.138	0.171	1.13	1.13	---	---	3.27	1.65	0.177
	Intermediate	.312	.202	.171	1.13	1.13	2.67	2.96	3.39	1.89	.177
	Small	.205	.309	.171	1.13	1.13	---	---	3.57	2.29	.177
10° Conical	Large	0.375	0.026	0.314	1.0	---	---	---	---	---	---
	Intermediate	.312	.090	.314	1.0	---	2.67	2.96	3.39	1.34	.218
	Small	.205	.197	.314	1.0	---	---	---	---	---	---

(b) Afterburner on; $A_8/A_m = 0.373$

		A_{pl}/A_m	A_{is}/A_m	A_{os}/A_m	A_{lip}/A_8	A_9/A_8 (b)	A_9/A_8 (c)	A_9/A_8 (d)	A_9/A_8 (e)	$\dfrac{A_{is} + A_{lip}}{A_8}$	$\dfrac{A_{os} + A_{lip}}{A_8}$
Cylindrical	Large	0.375	0.026	0.171	1.088	1.088	---	---	2.32	1.16	0.155
	Intermediate	.312	.090	.171	1.088	1.088	1.90	2.10	2.41	1.33	.155
	Small	.205	.197	.171	1.088	1.088	---	---	2.54	1.62	.155

[a]See fig. 5(a).
[b]$x/d_m = -0.16$.
[c]$x/d_m = 0.11$.
[d]$x/d_m = 0.35$.
[e]$x/d_m = 0.82$.
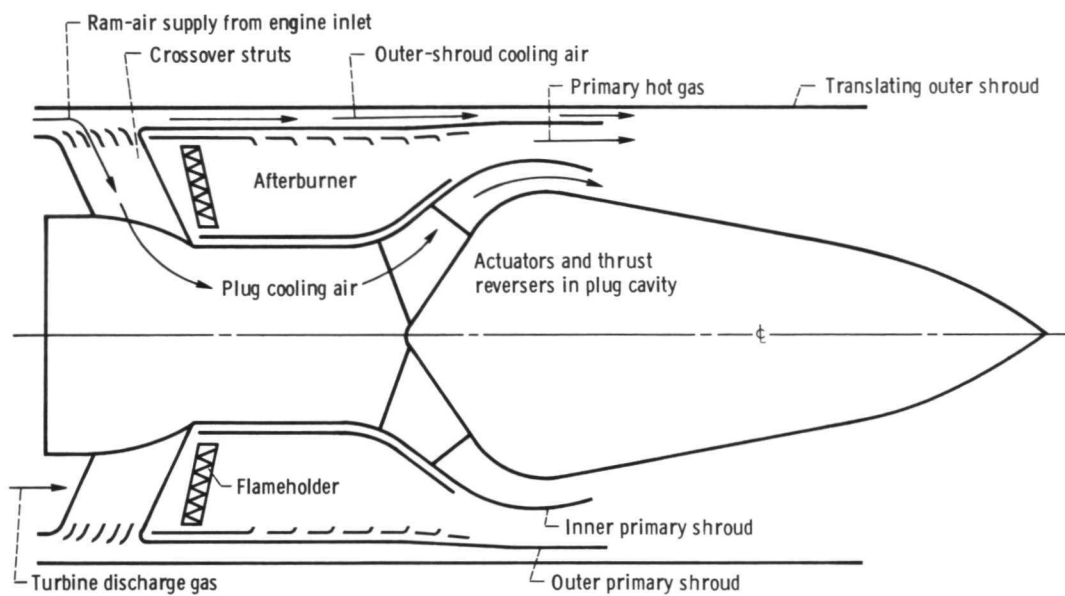
Figure 1. - Conceptual sketch of ram-air-cooled plug nozzle for typical large afterburning turbojet engine.

C-68-315
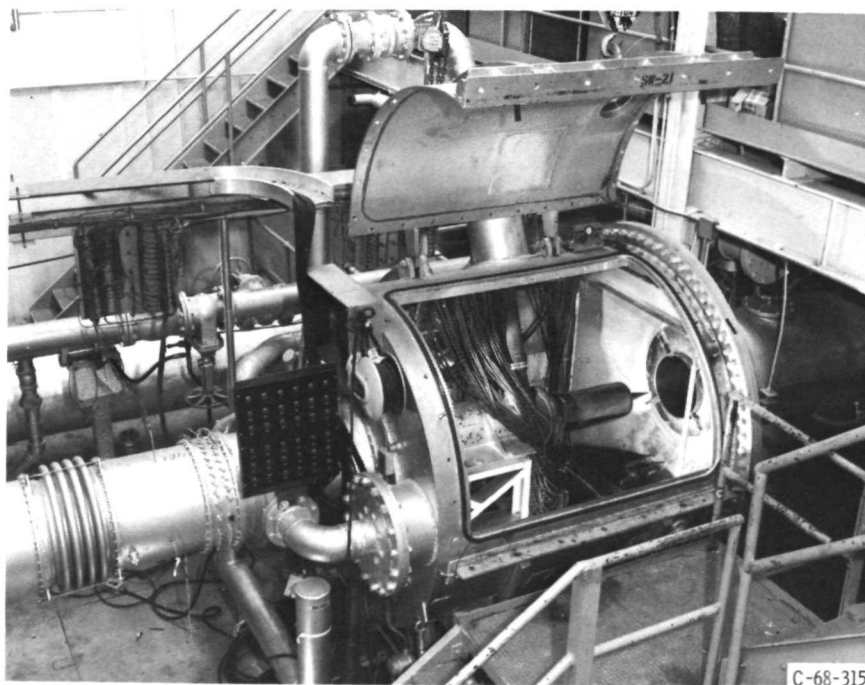
Figure 2. - Typical test nozzle installed in static test facility.
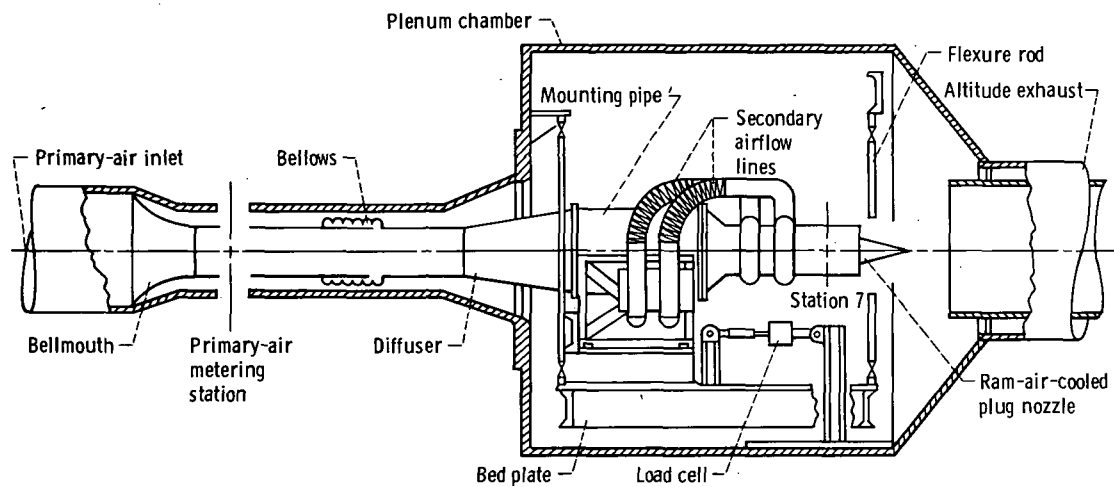
Figure 3. - Static test facility.

(a) Afterburner off. Standard deviation, σ, 0.0028.

(b) Afterburner on. Standard deviation, σ, 0.0018.
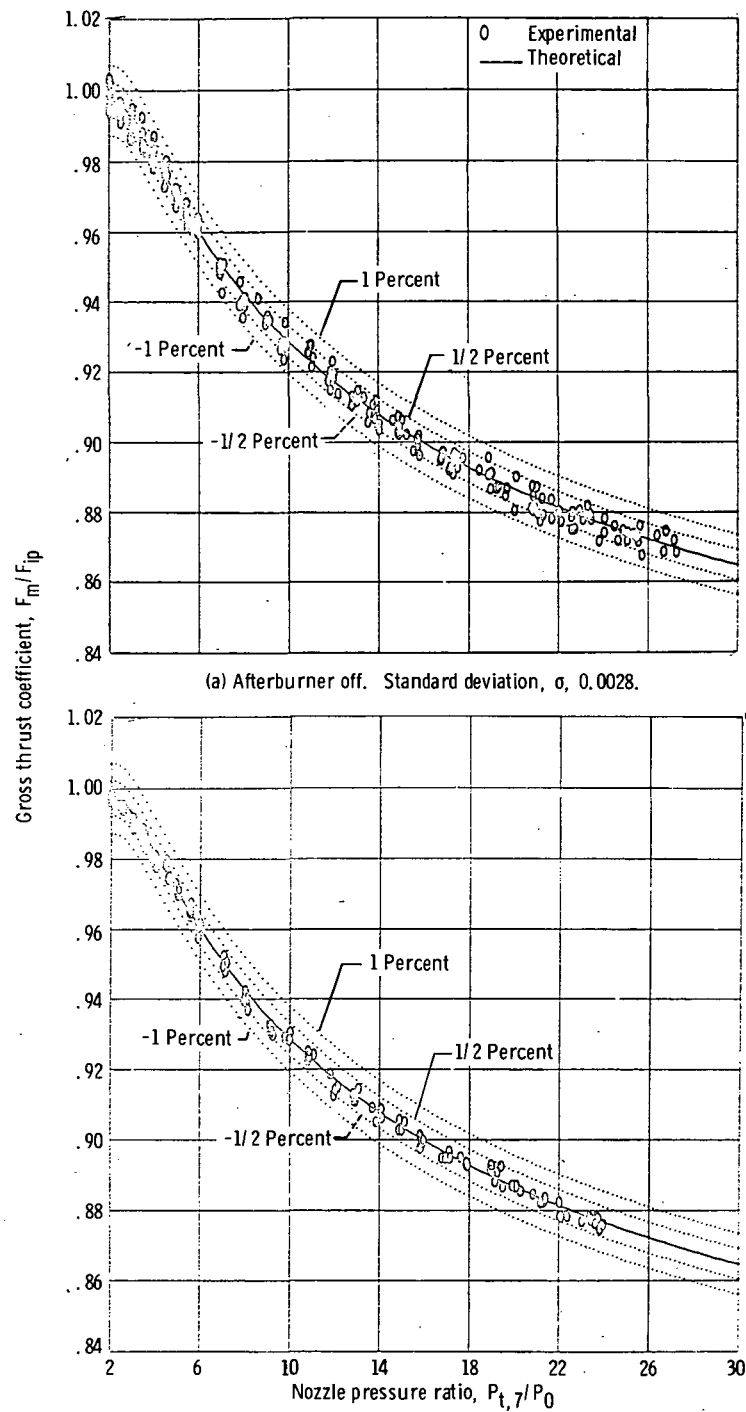
Figure 4. – Internal performance of ASME calibration nozzle.

Station 7
(x/d$_m$ = -0.74)

Station 8

Station 9

W$_{os}$

X

A$_{os}$

A$_8$

A$_{lip}$

W$_p$

A$_{is}$

A$_{pl}$

1.27 (0.50) rad.

35°

3.81
(1.50) rad.

9.769
(3.846)

10°

W$_{is}$

d$_m$ = 21.59
(8.50)

A

A

1.80
(0.71)

0.711
(0.280)

4.50
(1.77)

Section A-A

A$_9$

(a) Small plug.

Fully retracted
outer shroud

x/d$_m$ = -0.16

0.11   0.35

0.82

Fully extended
outer shroud

X

Plug support struts at
φ = 60°, 180°, and 300°

d$_m$ = 21.59
(8.50)

37.5°

3.81
(1.50) rad.

2.22
(0.875) rad.

12.055
(4.746)

10°

(b) Intermediate plug.

d$_m$ = 21.59
(8.50)

40°

3.81
(1.50) rad.

2.062
(0.812) rad.

13.223
(5.206)

10°

(c) Large plug.

Figure 5. – Plug geometric details. (All dimensions are in cm (in.).)
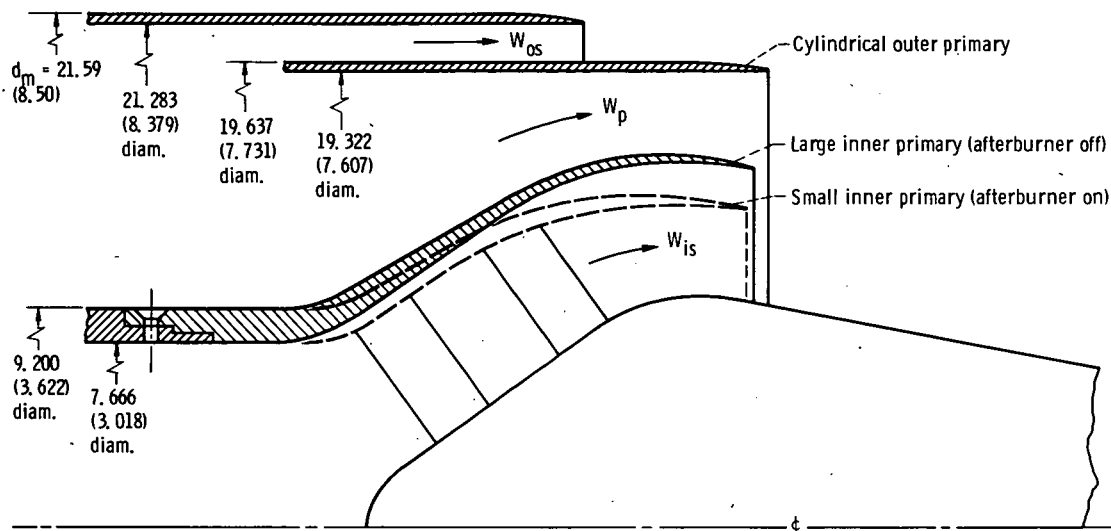
(a) Cylindrical outer primary with variable inner primary.
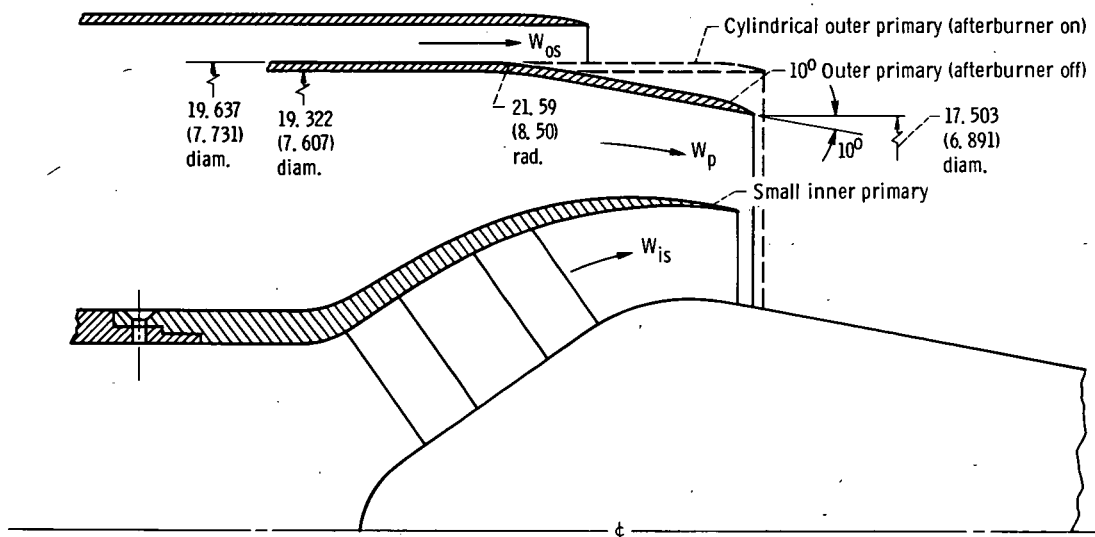
(b) Variable outer primary with small inner primary (10^0 outer primary and cylindrical outer primary).

Figure 6. - Primary nozzle configurations. (All dimensions are in cm (in.).)

5°   10°

2.39
(0.94)
rad.

30°

35°

9.50
(3.74)
rad.

14.115
(5.557)
diam.

13.556
(5.338)
diam.

Small inner primary

2.39
(0.94)
rad.

30°

35°

6.35
(2.50)
rad.

15.794
(6.218)
diam.

15.337
(6.038)
diam.

Large inner primary
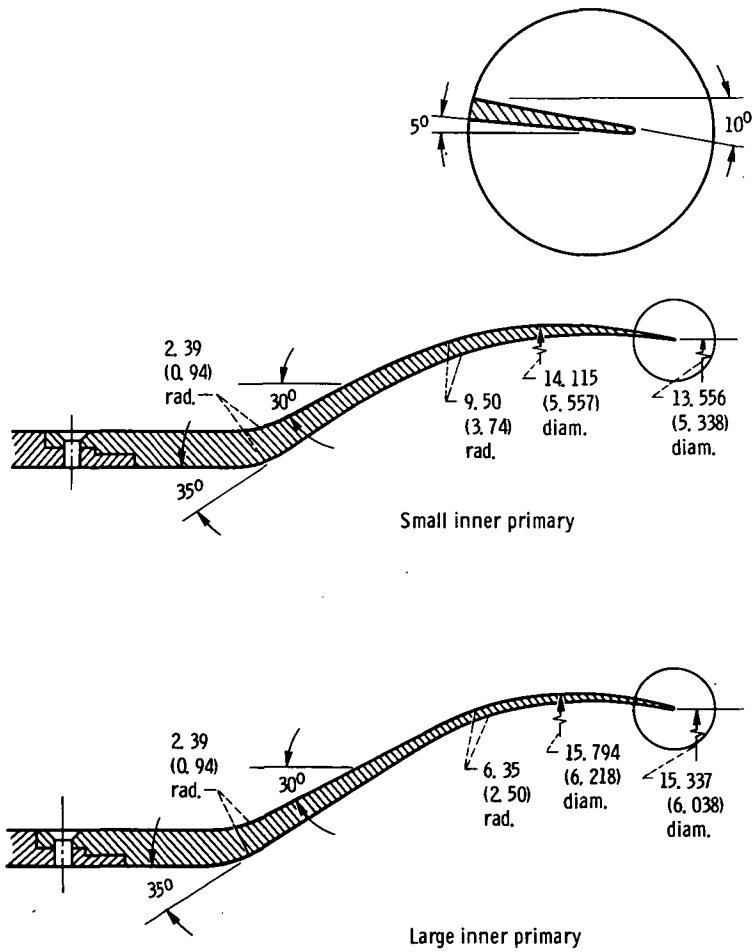
Figure 7. – Inner primary geometric details. (All dimensions are in cm (in.).)
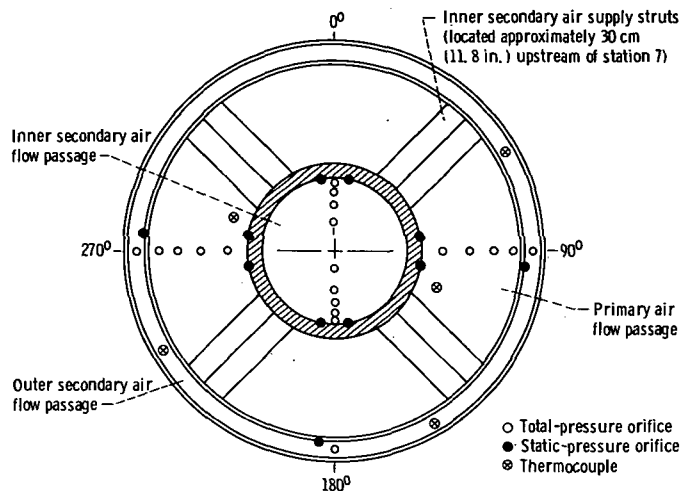
(a) Station 7 instrumentation (looking upstream).
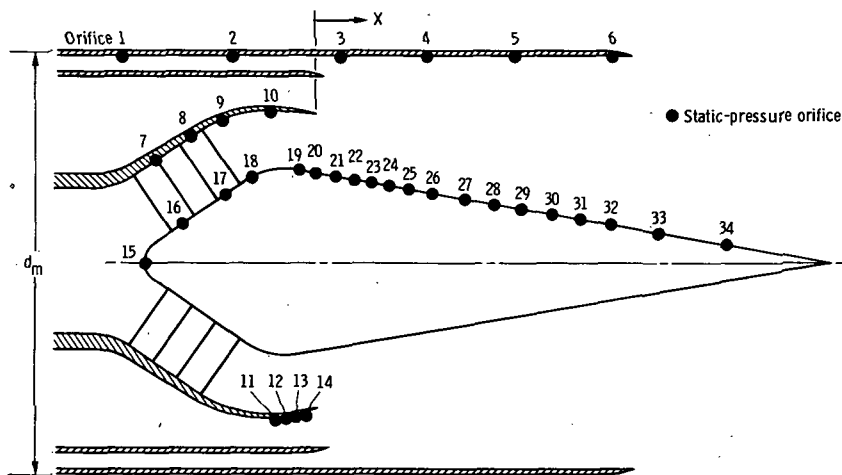
(b) Nozzle static-pressure instrumentation.

Orifice	Outer shroud, x/d_m
1	-0.478
2	-.188
3	.083
4	.318
5	.553
6	.789

Orifice	Small inner primary	Large inner primary
	Axial distance, X/d_m	
7	-0.384	-0.366
8	-.308	-.274
9	-.217	-.187
10	-.088	-.076
11	-.195	-.057
12	-.127	-.037
13	-.079	-.023
14	-.031	-.007

Orifice	Small plug	Intermediate plug	Large plug
	Axial distance, X/d_m		
15	-0.389	-0.393	-0.416
16	-.301	-.311	-.320
17	-.201	-.202	-.211
18	-.134	-.135	-.133
19	-.054	-.041	-.039
20	-.018	.004	.006
21	.026	.059	.065
22	.073	.115	.127
23	.121	.176	.191
24	.170	.238	.259
25	.223	.303	.331
26	.277	.371	.406
27	.336	.444	.484
28	.400	.520	.569
29	.467	.604	.661
30	.542	.696	.761
31	.623	.798	.874
32	.720	.915	1.004
33	.837	1.062	1.164
34	1.010	1.273	1.395

Figure 8. - Model instrumentation. (All dimensions are in cm (in.).)

$$F_c = F_p + F_{is} + F_{os} + F_{pl}$$
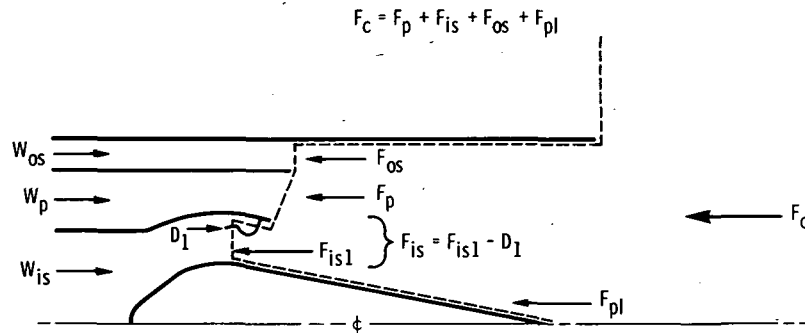
Figure 9. - Nozzle component force summary.

Nominal nozzle pressure ratio, $P_{t,7}/P_0$	Outer shroud length, x/d_m
○ 27	0.82
△ 4	-.16
□ 3	-.16

Plain symbols denote cylindrical outer primary
Tailed symbols denote 10^0 conical outer primary
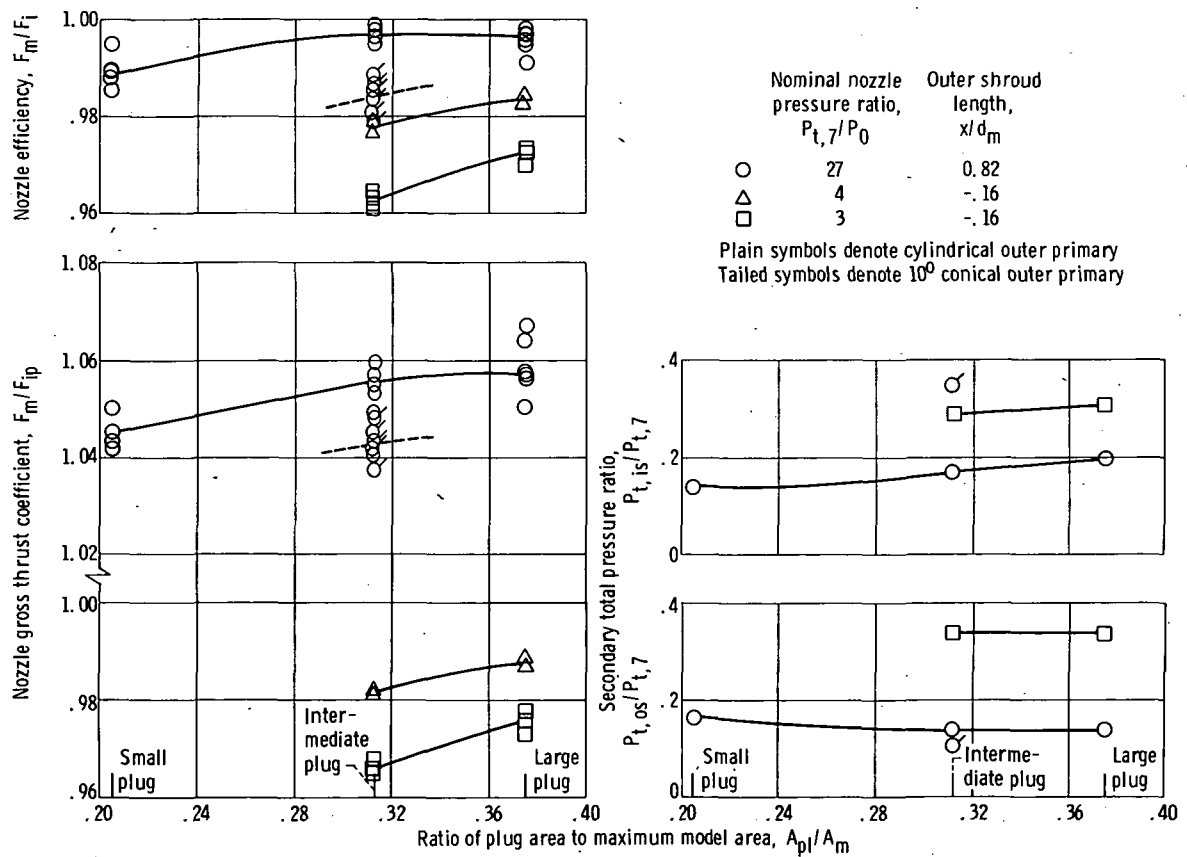
Figure 10. - Effect of plug size on nozzle performance characteristics. Afterburner off; corrected inner secondary weight flow ratio, 0.05; corrected outer secondary weight flow ratio, 0.03.
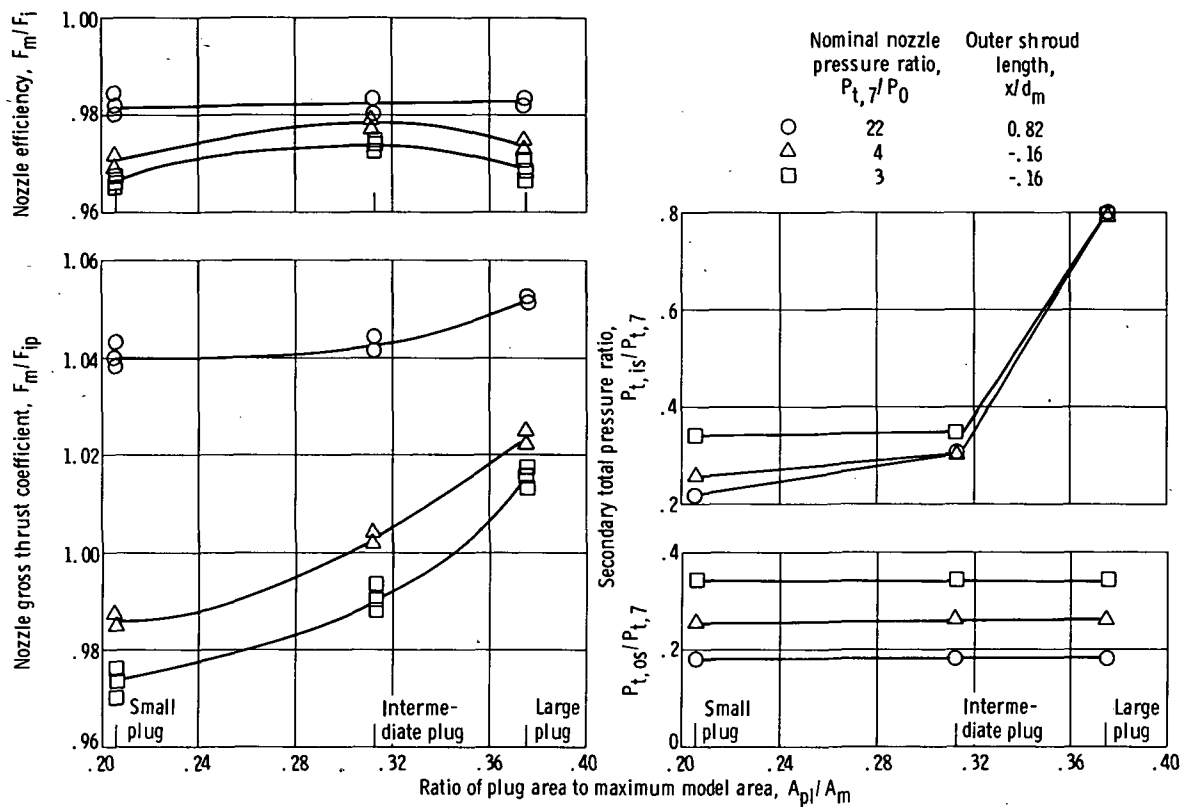
Figure 11. - Effect of plug size on nozzle performance characteristics. Afterburner on; corrected inner secondary weight flow ratio, 0.05; corrected outer secondary weight flow ratio, 0.03.

Nozzle efficiency

△ Measured, F_m/F_i (load cell measured)

□ Calculated, F_c/F_i (from pressure, temperature, and momentum)

● F_c adjusted to account for estimated internal friction

(a) Cylindrical outer primary.

(b) 10^0 Conical primary.
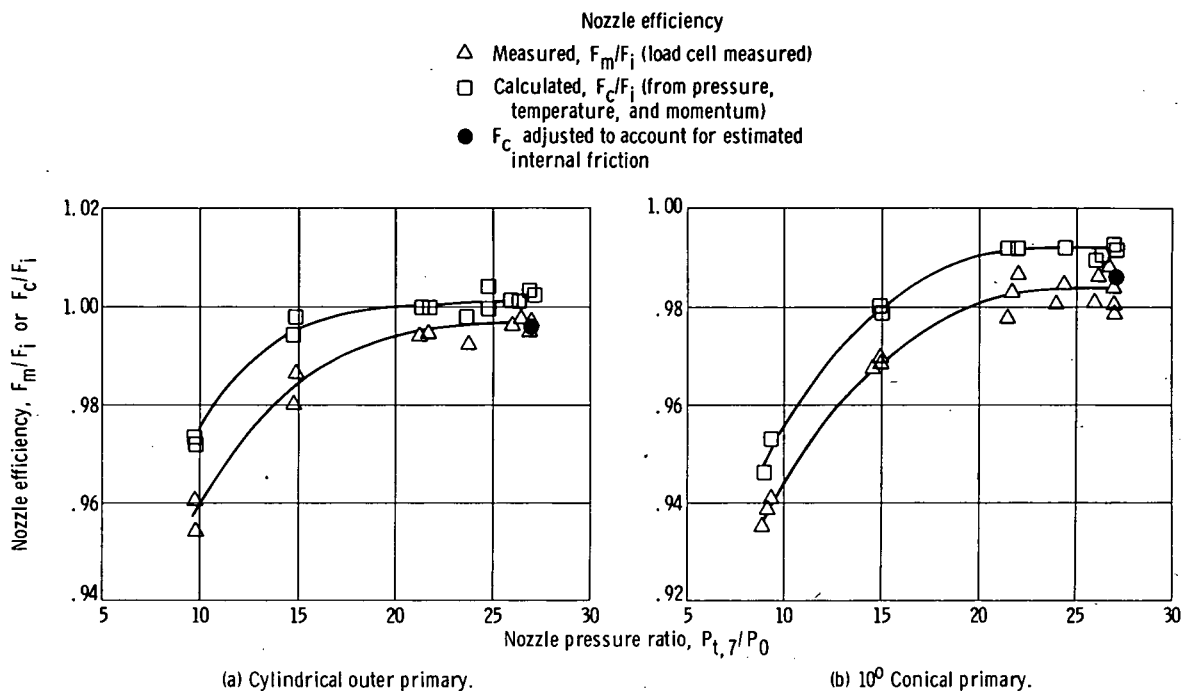
Figure 12. - Comparison of typical measured and calculated nozzle efficiencies. Afterburner off intermediate plug; fully extended outer shroud; corrected inner secondary weight flow ratio, 0.05; corrected outer secondary weight flow ratio, 0.03.

Plug size
○ Small
□ Intermediate
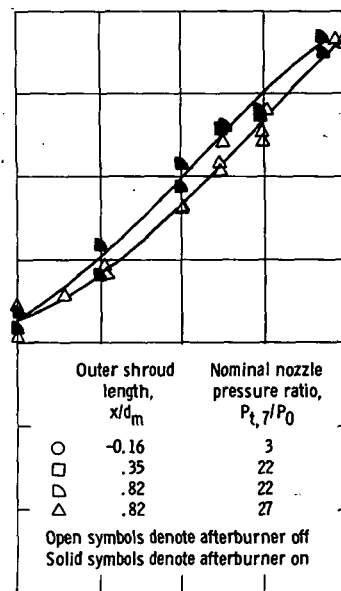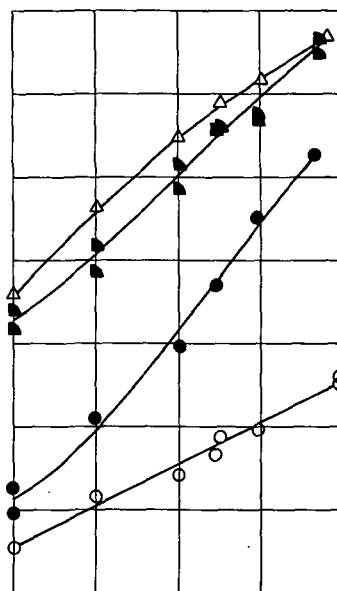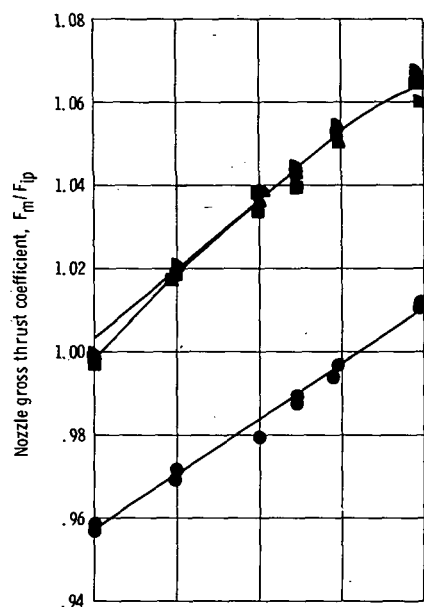◇ Large

(a) Afterburner off.

(b) Afterburner on.
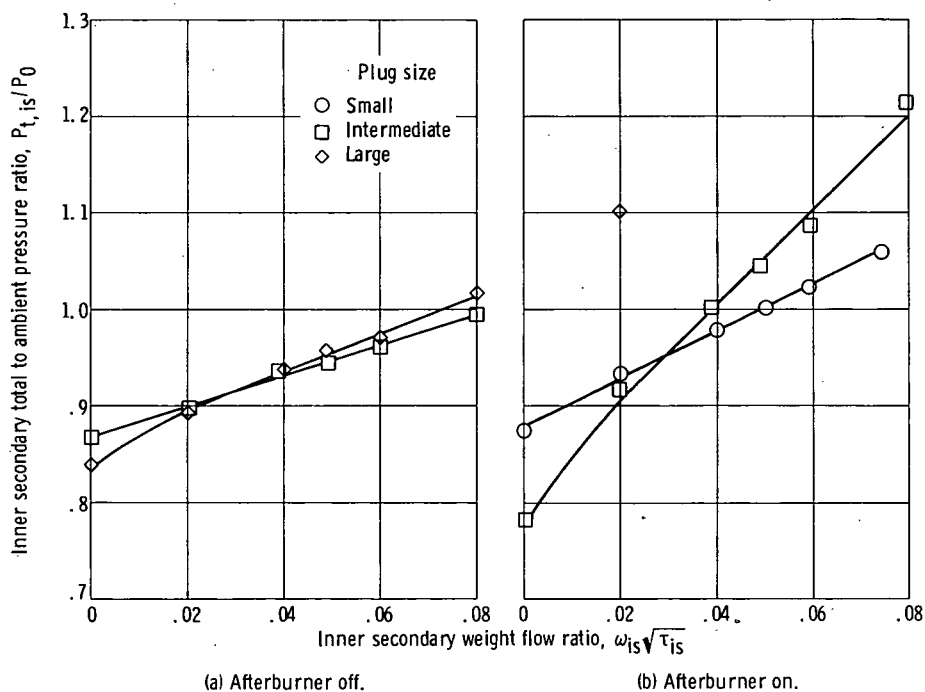
Figure 13. - Inner secondary flow pressure recovery requirements. Nozzle pressure ratio, 3.0; corrected outer secondary weight flow ratio, 0.03; fully retracted outer shroud.

Flagged symbols denote 10^0 conical outer primary
Plain symbols denote cylindrical outer primary

Afterburner on ← | → Afterburner off (cylindrical outer primaries)

Inner secondary weight flow ratio, $\omega_{is}\sqrt{\tau_{is}}$

0.08
.06
.04
.02
0

Secondary total pressure ratio, $P_{t,is}/P_{t,7}$

Area ratio, $(A_{is} + A_{lip})/A_8$
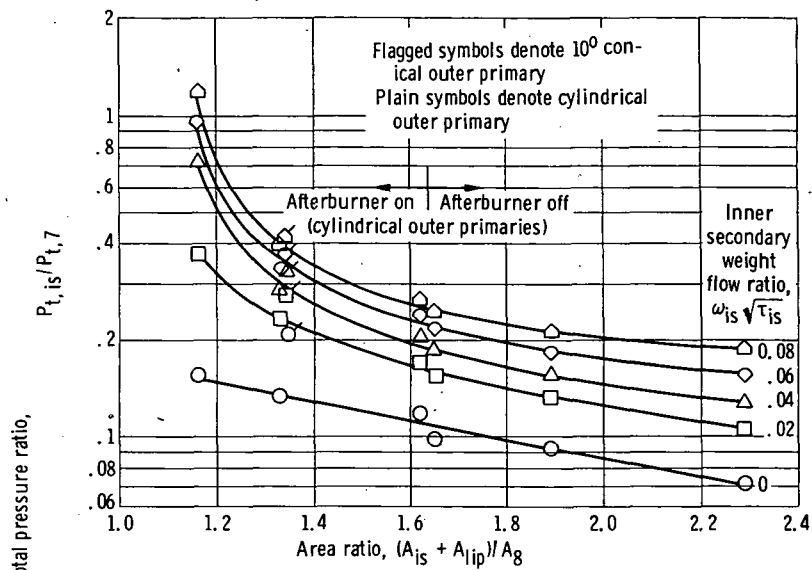
(a) Inner secondary. All outer shroud lengths.

Outer secondary weight flow ratio, $\omega_{os}\sqrt{\tau_{os}}$

0.06
.04
.03
.02

0

$P_{t,os}/P_{t,7}$

Area ratio, $(A_{os} + A_{lip})/A_8$
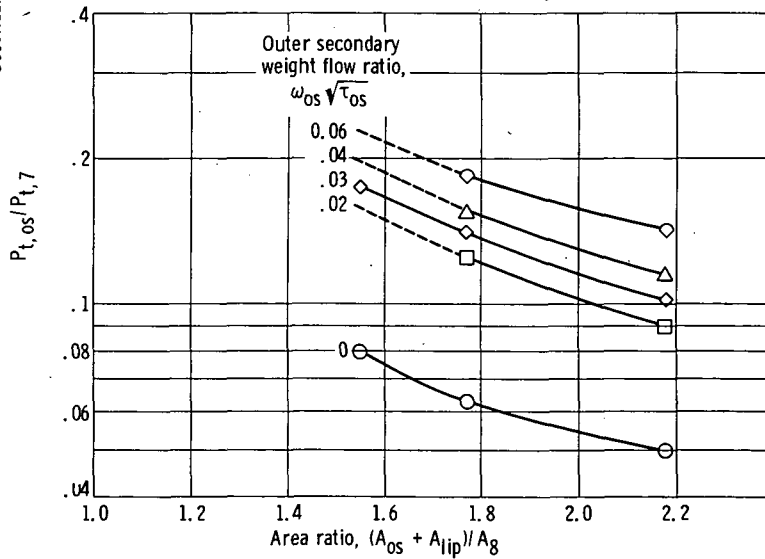
(b) Outer secondary. Outer shroud length, x/d_m, >0. 11; all plug sizes.

Figure 14. - Correlation of pumping characteristics with secondary and primary flow areas. High nozzle pressure ratio (>5.0).

27

Figure 16. - Correlation of pumping characteristics with secondary and primary flow areas. Inner secondary; low nozzle pressure ratio $\omega_{is}\sqrt{\tau_{is}} = 0.05$.

Figure 15. - Correlation of pumping characteristics with secondary and primary flow areas. Inner secondary; low nozzle pressure ratio ($P_{t7}/P_0 = 3$); fully retracted outer shroud.
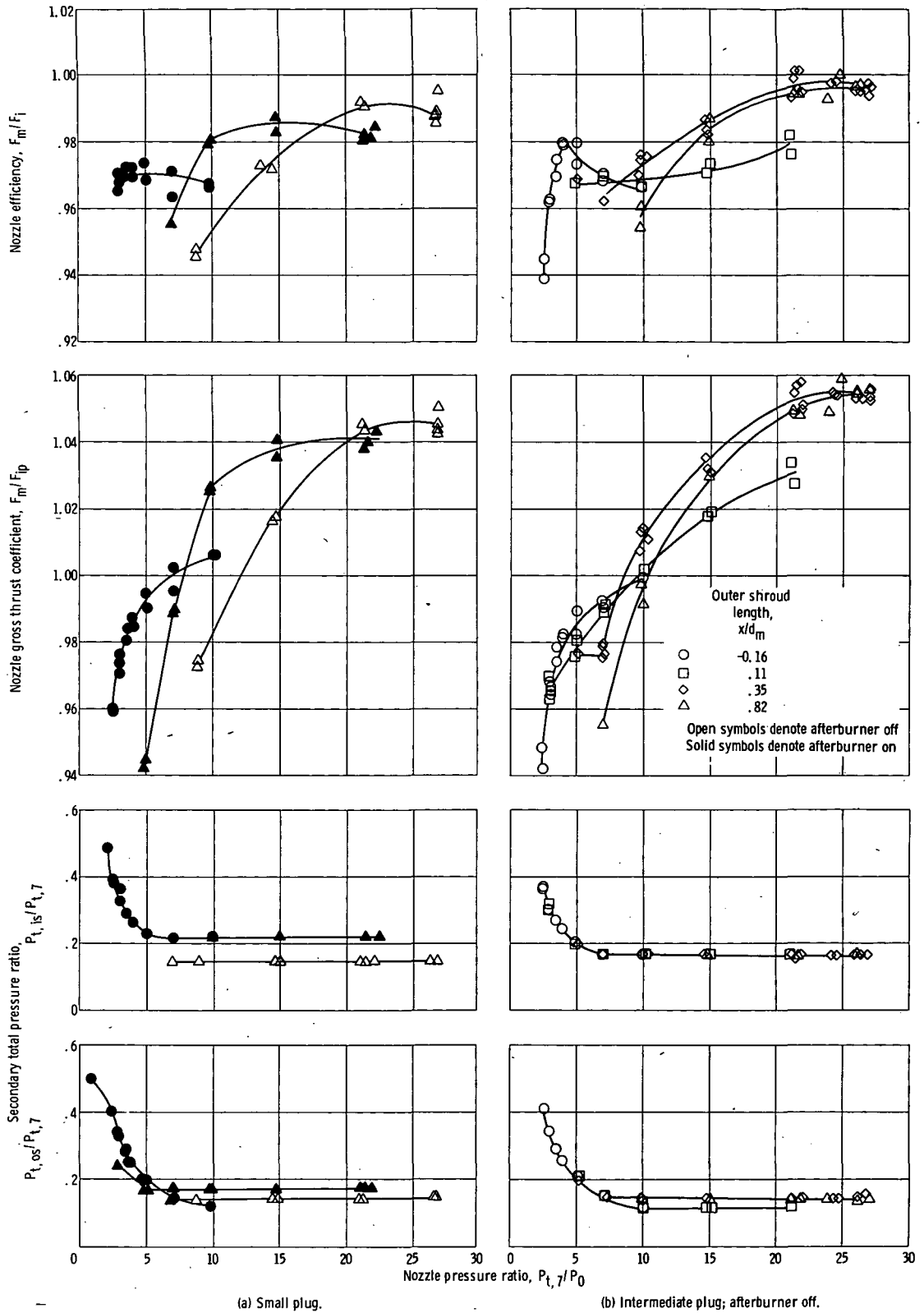
Figure 17. – Effect of outer shroud length on nozzle performance characteristics. Cylindrical outer primary; corrected inner-secondary weight flow ratio, 0.05; corrected outer secondary weight flow ratio, 0.03.

(a) Small plug.

(b) Intermediate plug; afterburner off.

29
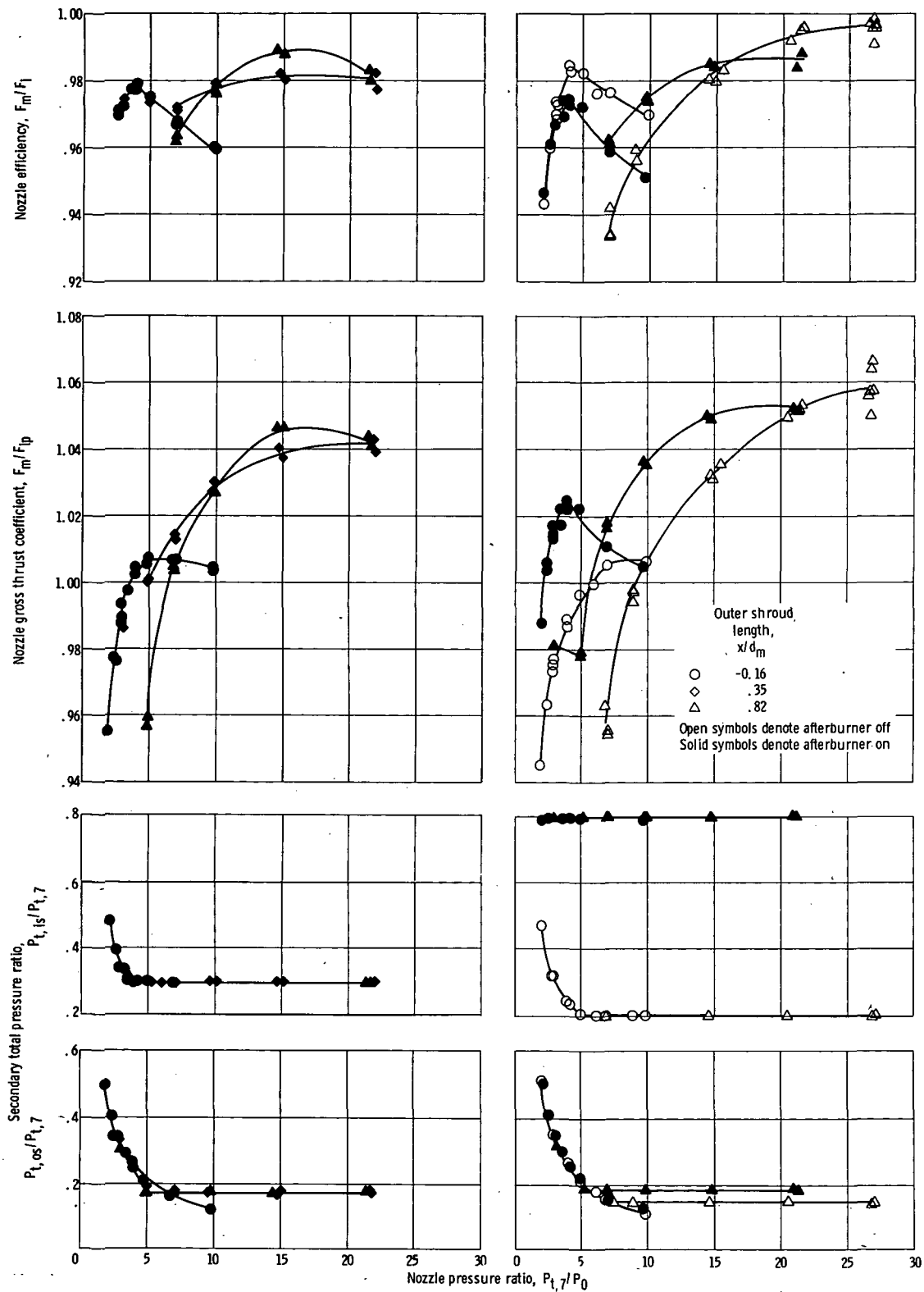
Figure 17. - Concluded.
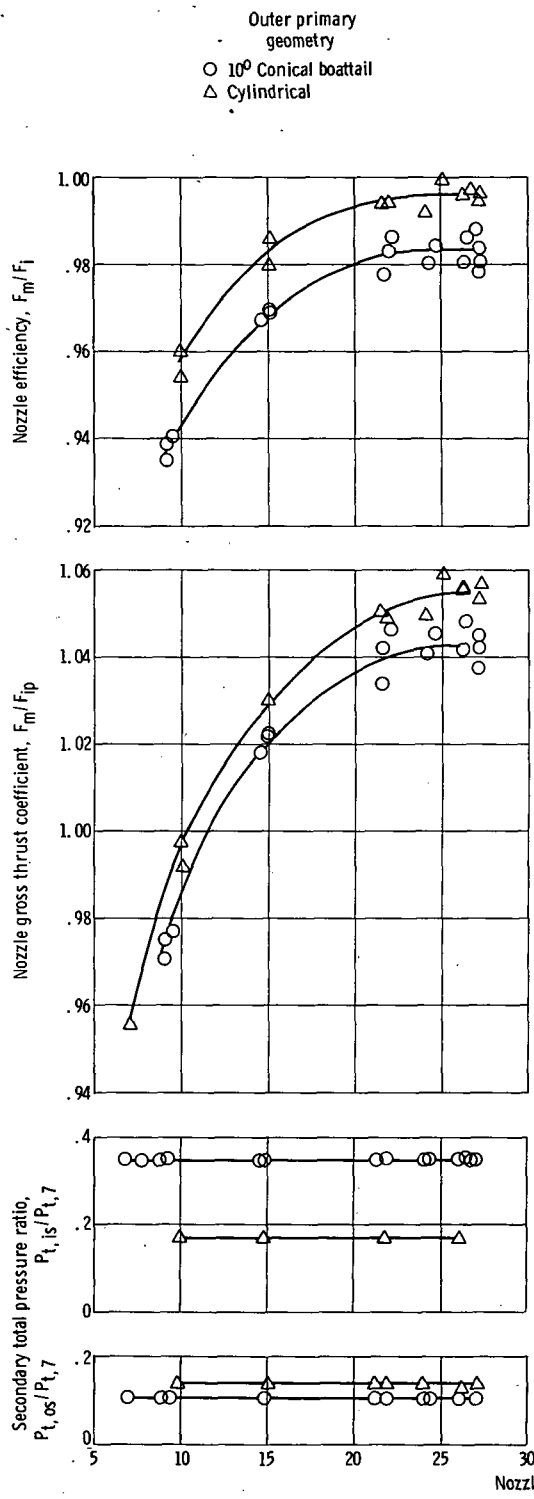
(a) Nozzle performance characteristics.
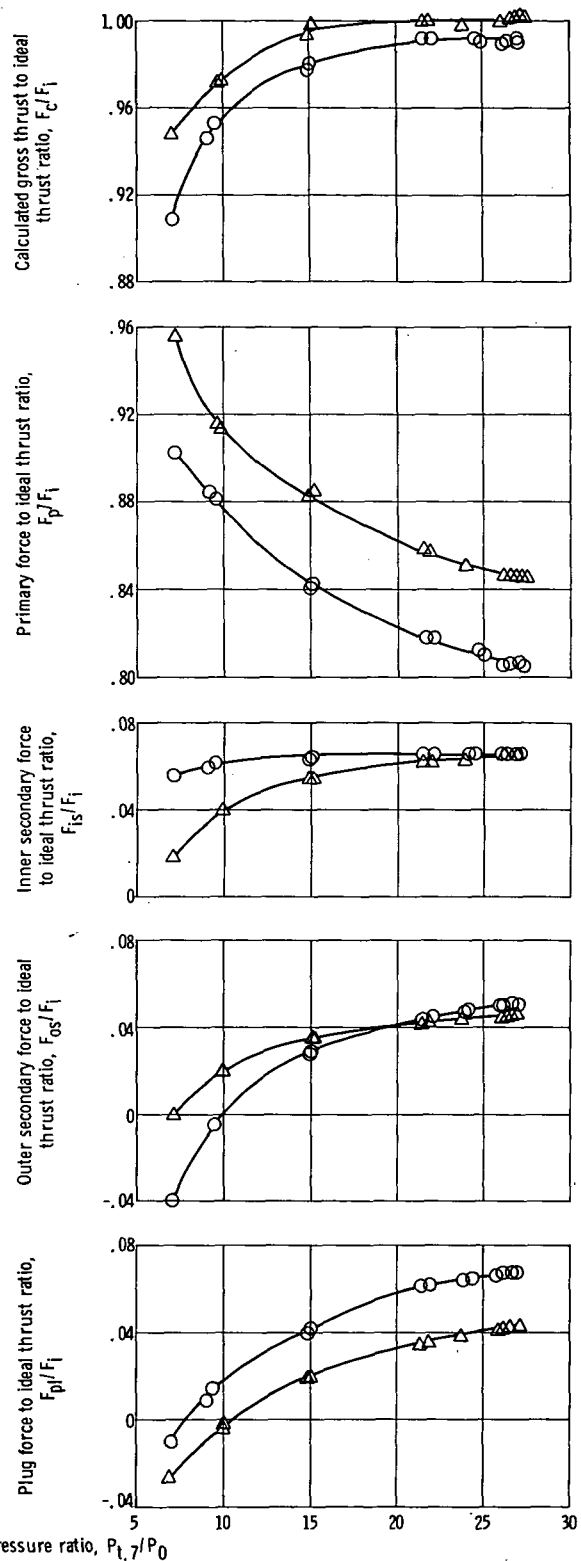
(b) Nozzle component forces. (Note: See fig. 9.)

Figure 18. – Effect of variable outer primary. Afterburner off, intermediate plug; outer shroud length, x/d_m, 0.82; corrected inner secondary weight flow ratio, 0.05; corrected outer secondary weight flow ratio, 0.03.
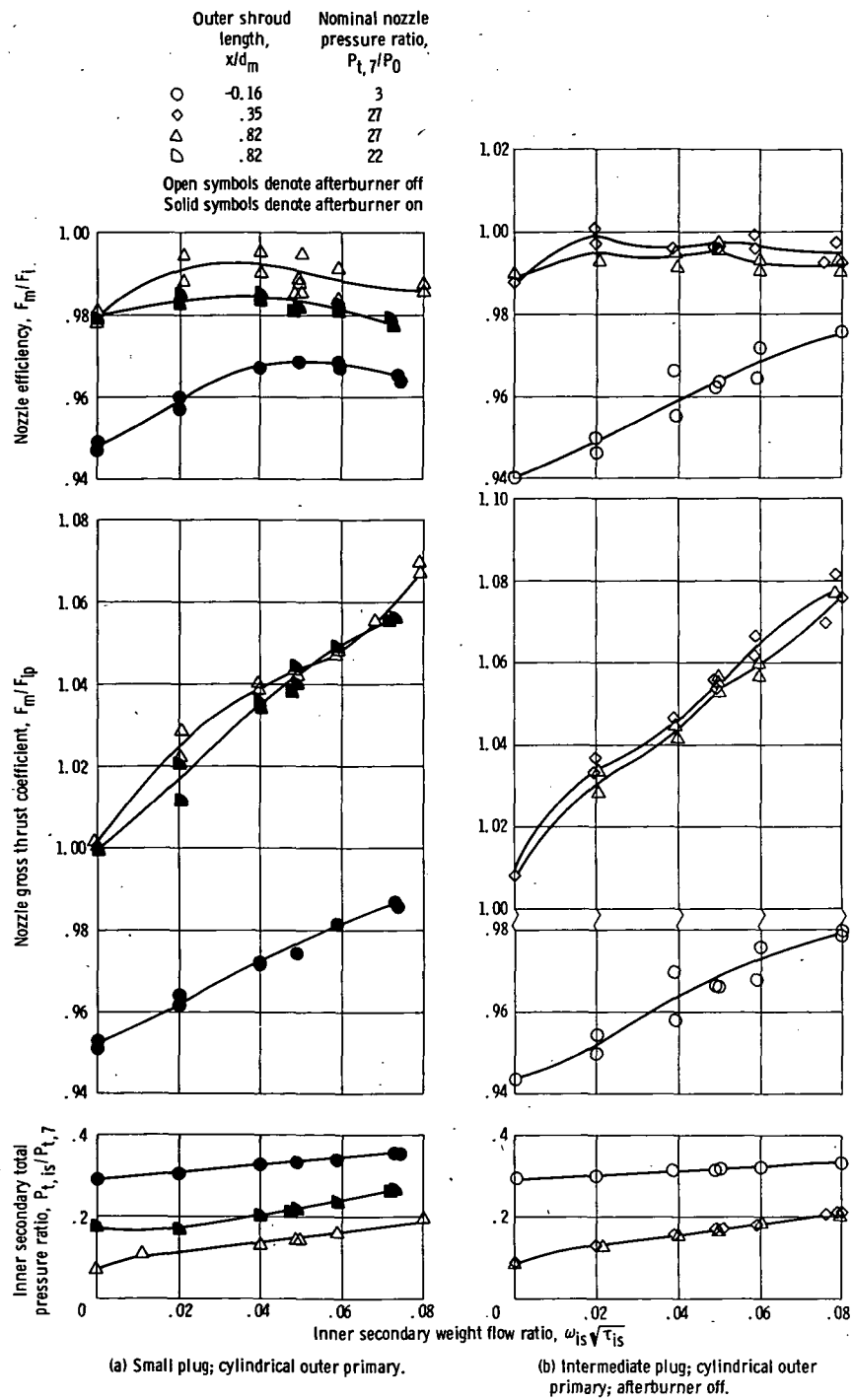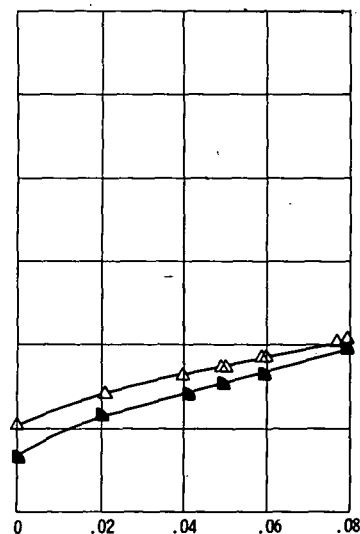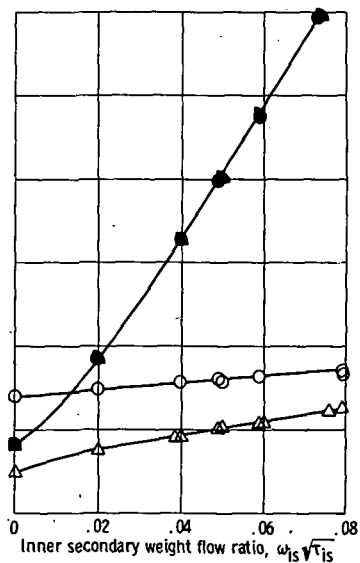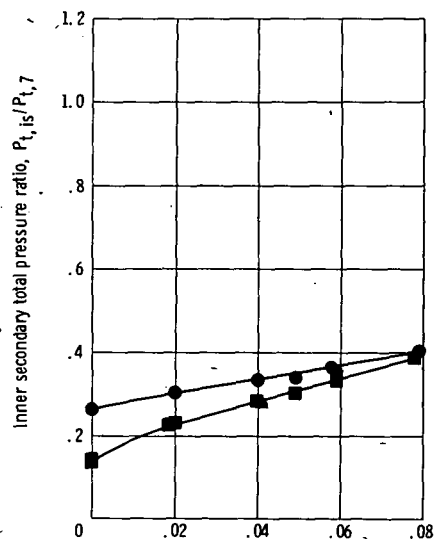
Figure 19. - Effect of inner secondary weight flow on nozzle performance characteristics. Corrected outer secondary weight flow ratio, 0.03.

Nozzle efficiency, F_m/F_i

1.00
.98
.96
.94

Nozzle gross thrust coefficient, F_m/F_{ip}

1.08
1.06
1.04
1.02
1.00
.98
.96
.94

Inner secondary total pressure ratio, $P_{t,is}/P_{t,7}$

1.2
1.0
.8
.6
.4
.2

0   .02   .04   .06   .08

Inner secondary weight flow ratio, $\omega_{is}\sqrt{\tau_{is}}$
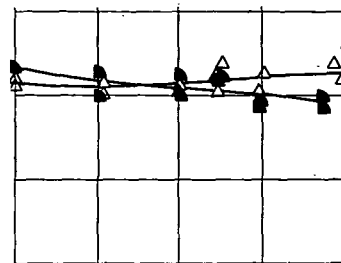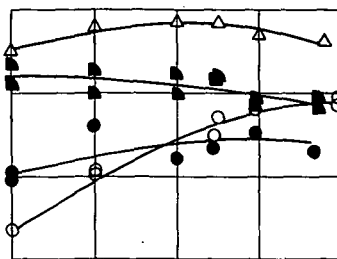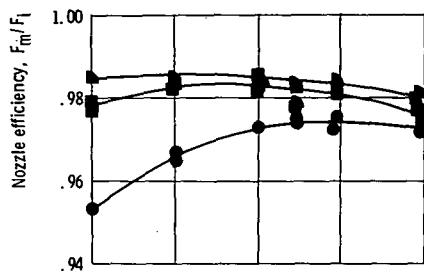
Outer shroud length, x/d_m	Nominal nozzle pressure ratio, $P_{t,7}/P_0$
O -0.16	3
□ .35	22
◁ .82	22
△ .82	27

Open symbols denote afterburner off
Solid symbols denote afterburner on

(c) Intermediate plug; cylindrical outer primary; afterburner on.

(d) Large plug; cylindrical outer primary.

(e) Intermediate plug; 10^0 conical outer primary (afterburner off) or cylindrical outer primary (afterburner on).
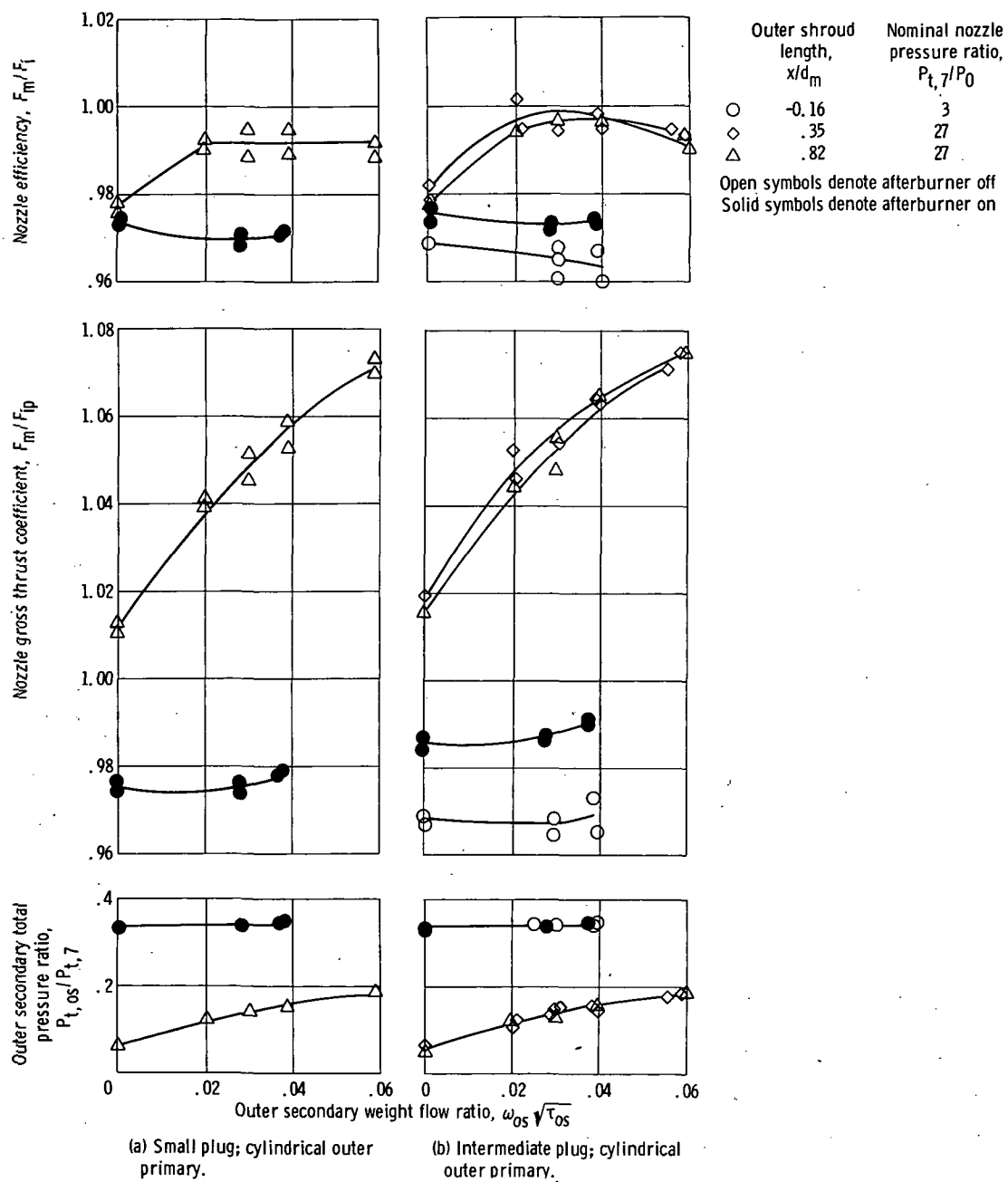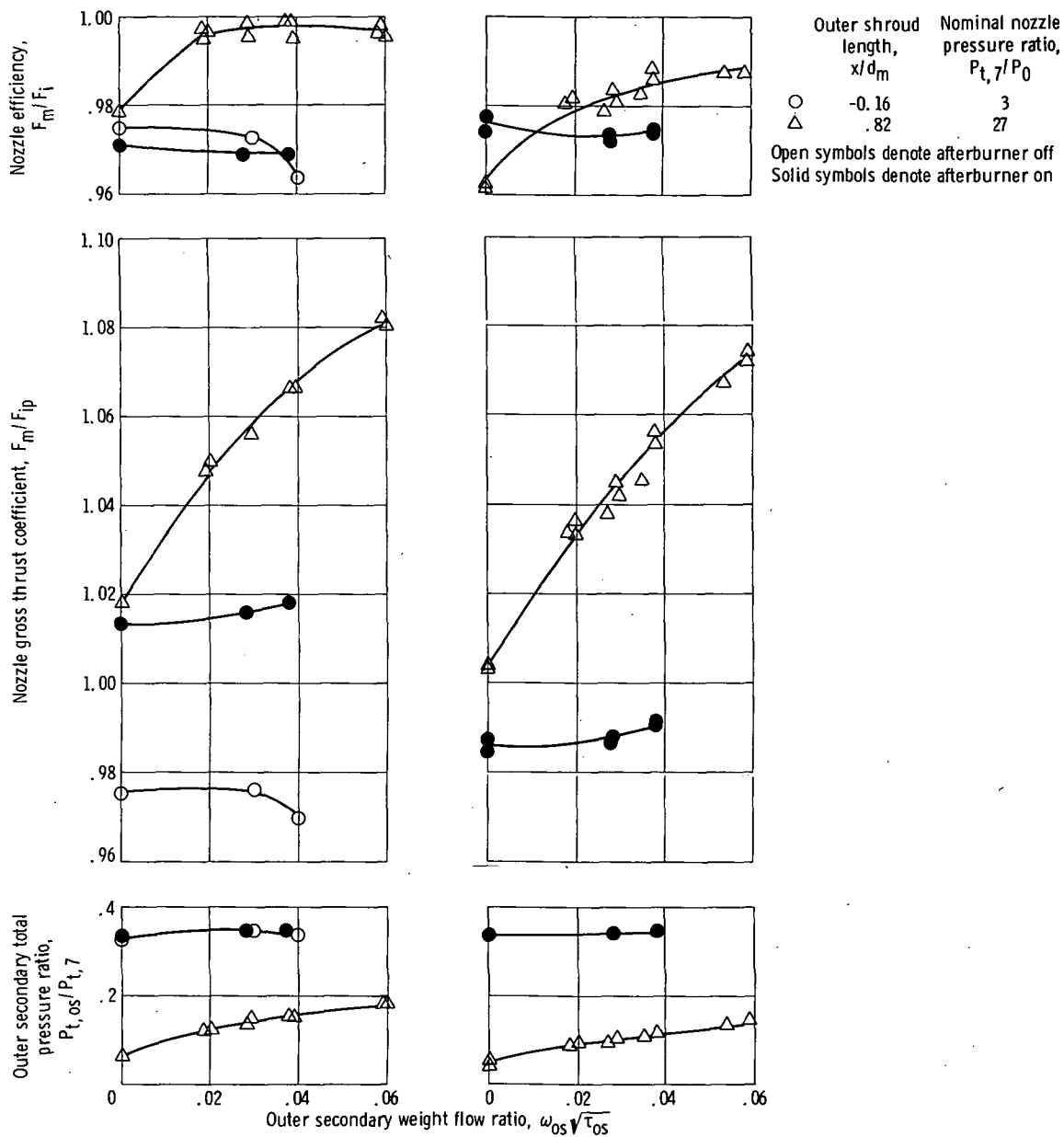
Figure 19. - Concluded.

33

Figure 20. – Effect of outer secondary weight flow on nozzle performance characteristics. Corrected inner secondary weight flow ratio, 0.05.

Figure 20. – Concluded.

"The aeronautical and space activities of the United States shall be conducted so as to contribute . . . to the expansion of human knowledge of phenomena in the atmosphere and space. The Administration shall provide for the widest practicable and appropriate dissemination of information concerning its activities and the results thereof."
—NATIONAL AERONAUTICS AND SPACE ACT OF 1958

NASA SCIENTIFIC AND TECHNICAL PUBLICATIONS

TECHNICAL REPORTS: Scientific and technical information considered important, complete, and a lasting contribution to existing knowledge.

TECHNICAL NOTES: Information less broad in scope but nevertheless of importance as a contribution to existing knowledge.

TECHNICAL MEMORANDUMS: Information receiving limited distribution because of preliminary data, security classification, or other reasons. Also includes conference proceedings with either limited or unlimited distribution.

CONTRACTOR REPORTS: Scientific and technical information generated under a NASA contract or grant and considered an important contribution to existing knowledge.

TECHNICAL TRANSLATIONS: Information published in a foreign language considered . to merit NASA distribution in English.

SPECIAL PUBLICATIONS: Information derived from or of value to NASA activities. Publications include final reports of major projects, monographs, data compilations, handbooks, sourcebooks, and special bibliographies.

TECHNOLOGY UTILIZATION PUBLICATIONS: Information on technology used by NASA that may be of particular interest in commercial and other non-aerospace applications. Publications include Tech Briefs, Technology Utilization Reports and Technology Surveys.

Details on the availability of these publications may be obtained from:

SCIENTIFIC AND TECHNICAL INFORMATION OFFICE

NATIONAL AERONAUTICS AND SPACE ADMINISTRATION

Washington, D.C. 20546